JOURNAL OF APPLIED ELECTROCHEMISTRY **27** (1997) 1172–1178

Characterization of *N*,*N*′-dimethyl-3,4,9,10-perylenetetracarboxylic acid diimide and phthalocyaninatozinc(II) in electrochemical photovoltaic cells

T. OEKERMANN, D. SCHLETTWEIN*

Institut für Angewandte und Physikalische Chemie, Universität Bremen, Fachbereich 2 (Biologie/Chemie), Postfach 330 440, 28334 Bremen, Germany

D. WÖHRLE

Institut für Organische und Makromolekulare Chemie, Universität Bremen, Fachbereich 2 (Biologie/Chemie), Postfach 330 440, 28334 Bremen, Germany

Received 16 September 1996; revised 20 December 1996

As a direct comparison to all-solid state photovoltaic cells, photoelectrochemical cells consisting of n-type *N*,*N*′-dimethyl-3,4,9,10-perylenetetracarboxylic acid diimide (MePTCDI) and p-type phthalocyaninatozinc(II) (PcZn) thin film electrodes vapour-deposited onto ITO have been investigated in aqueous ferri/ferrocyanide, *p*-benzoquinone/hydroquinone or I^{3-}/I^{-} electrolytes. The ferri/ferrocyanide cell has been studied in more detail, and the results are discussed with regard to the HOMO-, LUMO- and Fermi-energies of the materials used. A setup of the electrodes in a tandem cell could increase the efficiency of the cell due to improved light harvesting. Saturation of the photocurrent with increasing ferri/ferrocyanide electrolyte concentration at single PcZn or MePTCDI electrodes is discussed using a model of reactant adsorption prior to the charge transfer step. In addition, a decrease observed for the open-circuit voltage of the entire cell with increasing ferri/ferrocyanide concentration leads to an optimum concentration of 10^{-3} mol dm^{-3}.

Keywords: *photovoltaic cells, photoelectrochemical cells, vapour-deposited electrodes, PcZn thin films, MePTCDI thin films, electrode kinetics, adsorption*

1. Introduction

Thin films of organic pigments in general, and of 3,4,9,10-perylenetetracarboxylic acid derivatives and phthalocyanines in particular, show semiconducting properties. Many properties of the molecules, however, are preserved in the solid state, which led to their description as molecular semiconductors [1]. Their conduction type as a result of redox reactions with ambient molecules is defined by their frontier orbital positions and the materials can therefore be divided into p-type and n-type semiconductors. This is derived from photoelectrochemical experiments as well as from conductivity and thermopower measurements as compared to results of photoelectron spectroscopy [2–5]. In junctions with other semiconducting layers or with an appropriate electrolyte photovoltages and photocurrents can be obtained which opened the way to study the use of such films for solar energy conversion. Up to now the best results for organic solar cells were obtained from all-solid state p–n-cells containing phthalocyanines (Pc) as p-type semiconductor and perylenetetracarboxylic acid diimides (PTCDI) as n-type semiconductor in a configuration ITO/PTCDI/Pc/Au [5, 6]. Efficiencies up to $\eta = 0.43\%$ and fill factors up to $FF = 0.32$ were reported for such cells of phthalocyaninatozinc(II) (PcZn) and *N*,*N*′-dimethyl-3,4,9,10-perylenetetracarboxylic acid diimide (MePTCDI), with short-circuit currents $I_{SC} \leq 3.53$ mA cm^{-2} and open-circuit voltages $V_{OC} \leq 415$ mV [6]. These results are due to a good harvest of the visible light, because both classes of materials have intense absorption maxima (absorption constant per unit film thickness, $\alpha \leq 10^5$ cm^{-1}) in the visible region, complementing one another (Fig. 5).

In photoelectrochemical experiments cathodic photocurrents were observed at the surface of PcZn as typical for p-type semiconductors [7, 8]. MePTCDI behaved as n-type semiconductor in contact to various electrolytes, and anodic photocurrents were observed [9, 10]. Both materials showed a significant chemical and thermal stability in photoelectrochemical experiments [10, 11]. For photoelectro-

* Author to whom correspondence should be addressed.

0021-891X

chemical solar cells of Pc, for example PcTiO [12] and PcAlCl [13], some photovoltaic parameters were reported with efficiencies not exceeding 0.08%. All these cells consisted of only one semiconductor electrode and a metal counter electrode in a reversible electrolyte, corresponding to Schottky cells, in which a semiconductor and a metal are in direct contact.

In this paper we report on photoelectrochemical cells consisting of PcZn and MePTCDI corresponding to the p–n-cells as mentioned above. In contrast to p–n-junctions, in which crystallographic strain in the interface of the materials would be expected, leading to small interfacial contact area and efficiency losses due to trapping and recombination in crystal defect centres, the semiconductor/electrolyte interface of a photoelectrochemical cell avoids this organic/organic solid contact and provides large contact area at the surfaces. Because of the high transparency of ITO (indium tin oxide) for visible light, a cell configuration ITO/MePTCDI/electrolyte/PcZn/ITO was chosen, so that all electrodes can be illuminated from both sides alternatively. Furthermore both electrodes of a cell can be placed in a tandem arrangement and illuminated in series to obtain a good light harvesting. As electrolytes we use aqueous solutions of ferri/ferrocyanide, *p*-benzoquinone/hydroquinone and I_3^-/I^-. The kinetics of charge transfer at the electrodes are studied in detail, the rate-limiting steps of the surface-reactions are identified and the mechanism is discussed.

2. Experimental details

2.1. *Electrode preparation*

PcZn was purchased from Aldrich and MePTCDI was obtained from Hoechst. Both pigments were purified by zone sublimation. All other chemicals used in this study were purchased in analytical grade and used without further purification. ITO with an average transmission of 85–90% in the visible region was purchased from Flachglas and cut into plates of 1.5 cm^2. The PcZn and MePTCDI films were vapour-deposited (thickness: 100 nm) on the ITO substrate (25 °C) at 10^{-5} torr with a deposition rate of 0.2 nm s^{-1}. UV–vis spectra of the thin films were recorded by a Perkin–Elmer Lambda 2 spectrometer. The electrodes were contacted by a glass covered copper wire using conductive adhesive Ecobond 57C from Grace leaving a square of 1 cm^2 active area. The connections and the non active electrode area were sealed with Araldide Rapid epoxy resin from Ciba Geigy.

2.2. *Photoelectrochemical measurements*

The experiments were performed in three different geometrical and electrical arrangements: (i) as single working electrodes in a typical three-electrode setup; (ii) in a U-tube cell with the two electrodes serving as anode and cathode of the cell; (iii) in a tandem cell with the light passing through the anode and cathode consecutively. The first two sets of experiments were conducted in a U-shaped glass tube with an inside diameter of 2 cm. The two half cells were divided by a ceramic frit in the centre of the U to separate different electrolytes if necessary and each contained one electrode. Cyclic voltammograms (CV) with single semiconductor electrodes were performed with the working electrode, connected to a saturated calomel reference electrode (SCE) by a salt bridge, in one half cell and an uncovered ITO counter electrode in the other half cell. In the second experiment (U-tube cell) each semiconductor electrode was placed in one half-cell of the U-tube and measured against each other. To allow better light harvesting two electrodes of PcZn and MePTCDI were prepared as a tandem cell: both electrodes, parallel and with the thin films faced to each other at a distance of 0.5 cm, were fixed on a glass plate with epoxy resin together with two other glass plates as lateral walls.

Aside from the third arrangement the electrodes could be illuminated separately by 150 mW halogen lamps from Reflecta through water filters. The incident light intensity at the electrodes was 96 mW cm^{-2}, measured with a Kipp & Zonen A1-754399 instrument. The light intensity could be reduced by neutral density filters from Melles Griot with optical densities between 0.1 and 1. Photocurrents were calculated as the difference between the overall current under illumination and the dark current. Photocurrent spectra were measured with metal interference filters from LOT with a stepwidth of 20 nm and a bandwidth of 10 nm. Electrolyte concentration dependent measurements with ferri/ferrocyanide solutions were carried out with 460 nm cut-off filters instead of water filters to avoid an influence of light absorption in the electrolyte. If not mentioned otherwise all experiments were performed in an aqueous 1 mol dm^{-3} KCl solution.

V_{OC} was measured using a Jaissle FET-K10 millivoltmeter with an input resistance of $10^{14}\Omega$. I_{SC} and current–voltage curves were measured with a Jaissle 1003 T-NC potentiostat connected to a Wenking VSG 83 voltage scan generator and to a Philips PM 8272 *XYt*-recorder. In cell arrangements the direction of currents and potentials are referred to the PcZn electrode. To obtain current–voltage curves comparable to the curves of all-solid state cells both branches of the measured CV were averaged to give functions of current on voltage, and efficiencies and fill factors were calculated from the averaged curves. The efficiency, η, is obtained by dividing the maximum power output by the incident light power, Φ (Equation 1). The fill factor, *FF*, is given according to Equation 2, where I_{max} and V_{max} are the current and voltage corresponding to the maximum power output.

$$\eta = (V_{OC} I_{SC} FF)/\Phi \quad (1)$$

$$FF = (V_{max} I_{max})/(V_{OC} I_{SC}) \quad (2)$$

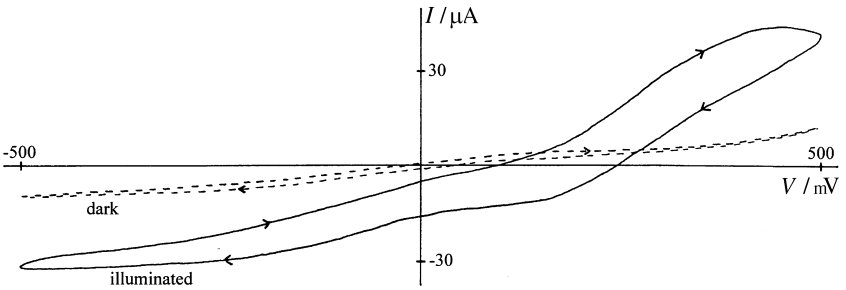

Fig. 1. Current voltage curves in the dark (– – –) and under illumination with 96 mW cm^{-2} white light (——) of a photoelectrochemical cell (U-tube cell) consisting of a PcZn electrode in one half cell and a MePTCDI electrode in the other half cell with a ferri/ferrocyanide electrolyte ($c = 10^{-3}$ mol dm^{-3}). The current direction and the voltage are given for the PcZn electrode.

3. Results

Figure 1 shows the current–voltage curve observed for the polarization of a photoelectrochemical cell (U-tube cell) consisting of an illuminated PcZn electrode in one half-cell and an MePTCDI electrode in the other half-cell, both in a ferri/ferrocyanide electrolyte ($c = 10^{-3}$ mol dm^{-3}). Compared to the curve measured with both electrodes in the dark, which is also shown in Fig. 1, a significant photoeffect is obtained for both the cathodic (cathodic currents at PcZn, anodic currents at MePTCDI) and the anodic direction (vice versa). The ferri/ferrocyanide electrolyte produced the highest values of η and *FF* in comparison to *p*-benzoquinone/hydroquinone and I_3^-/I^- as shown in Table 1.

For cells containing reversible electrolytes the values of V_{OC} were nearly the sum of the values measured when one electrode remained dark, respectively. The illuminated MePTCDI electrode for example of the ferri/ferrocyanide cell in Table 1 generated a V_{OC} of 130 mV with the PcZn electrode in the dark. In the opposite case a V_{OC} of 55 mV was obtained. The replacement of a dark semiconductor electrode by ITO or Pt electrodes did not cause any changes in these values, which means that the resistance of the thin films causes no barrier concerning the photovoltage. On the other hand the photocurrents did not behave additively. I_{SC} measured with both electrodes illuminated (10.5 μA) was nearly double the sum of the values obtained when one electrode remained dark (4.8 μA when PcZn was dark, 1.4 μA when MePTCDI was dark), due to the high resistance of a dark semiconductor electrode and changes in charge transfer kinetics at the dark electrode compared to the same electrode when illuminated. The overall current I_{SC} cannot be higher than the current at the electrode with the slower kinetics under the established potential.

Table 1. Cell characteristics of ITO/PcZn/electrolyte/MePTCDI/ITO cells (U-tube cells) for different electrolytes (10^{-3} mol dm^{-3} except 0.5 mol dm^{-3} KI)

Electrolyte	I_{SC} /μA cm^{-2}	V_{OC} /mV	*Fill factor, FF*	*Efficiency, η* /%
$Fe(CN)_6^{3-}$ / $Fe(CN)_6^{4-}$	10.5	180	0.32	0.000 32
p-benzoquinone /hydroquinone	7.8	134	0.21	0.000 12
I_3^-/I^-	4.8	109	0.25	0.000 07

Both electrodes were illuminated with 96 mW cm^{-2} white light. KCl was used as supporting electrolyte ($c = 1$ mol dm^{-3}) except for I_3^-/I^- where KI functioned as supporting electrolyte

Current–voltage curves for single electrodes of MePTCDI and PcZn in a three-electrode setup were measured at different ferri/ferrocyanide concentrations in the dark and under illumination using 460 nm cut-off filters to exclude influences of absorption by the electrolyte. Some of the curves are depicted in Fig. 2. The photocurrents and the dark currents are plotted against the electrolyte concentration in Fig. 3 for PcZn at 50 mV vs SCE (cathodic currents) and for MePTCDI at 350 mV vs SCE (anodic currents). The dark currents increase linearly with the electrolyte concentration. Either limitation by charge transfer kinetics or charge transfer limited by diffusion would explain this behaviour. The non linear dependence on electrolyte concentration of the photocurrents, however, indicates that a surface reaction is involved which is discussed below.

Concentration dependent experiments in the entire cell (U-tube cell) without the cut-off filters, but with normal water filters showed that at higher electrolyte concentrations than 10^{-3} mol dm^{-3}, I_{SC} decreases due to the higher light absorption in the electrolyte (Table 2). The highest efficiency of 2.3×10^{-4}% was determined at an electrolyte concentration of

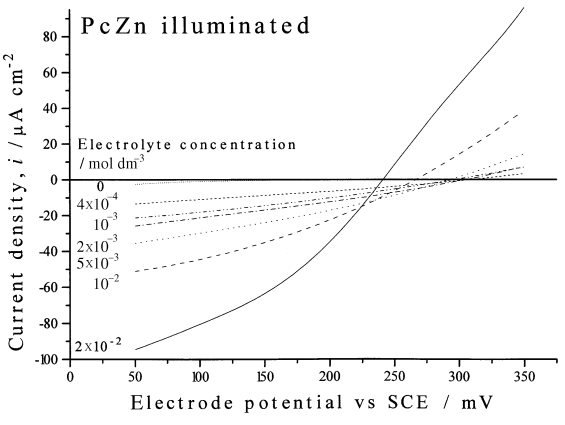

Fig. 2. Current–voltage curves measured in a three-electrode setup of an illuminated PcZn electrode for different ferri/ferrocyanide concentrations in the electrolyte. Illumination by 96 mW cm^{-2} white light through 460 nm cut-off filters.

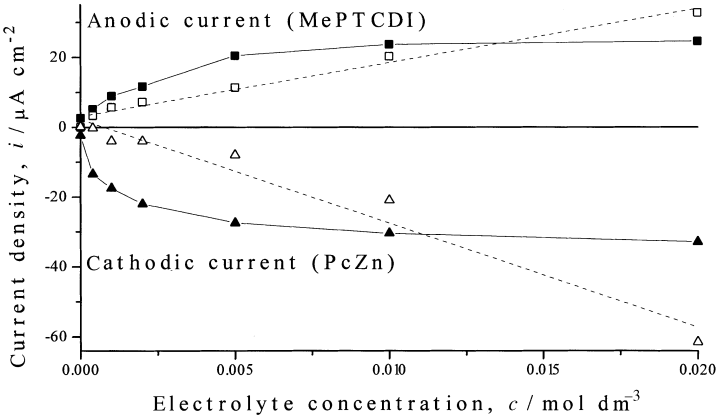

Fig. 3. Concentration dependence of the dark current density (– –△– –) and the photocurrent density under illumination with 96 mW cm^{-2} white light through 460 nm cut-off filters (—▲—) for a PcZn electrode at 50 mV vs SCE as well as for an MePTCDI electrode at 350 mV vs SCE in the dark (– – □ – –) and under the same illumination (—■—).

10^{-3} mol dm^{-3} due to the highest I_{SC} at this concentration.

V_{OC} and *FF* also decrease when the concentration is increased. The decrease in V_{OC} is not only caused by the higher light absorption in the electrolyte. In Fig. 4 the concentration dependence of the rest-potentials of PcZn and MePTCDI electrodes in the three-electrode arrangement can be seen. The difference between the electrolyte equilibrium potential (230 mV vs SCE) and the rest-potential of an electrode reflects its contribution to V_{OC} of a cell. Although cut-off filters were used, a decrease in V_{OC} with increasing electrolyte concentration is observed, which can be explained by increased recombination currents at higher electrolyte concentration.

The spectral dependence of I_{SC} has been investigated in the tandem cell. The absorption spectrum of the entire tandem cell, which is composed of the single absorption spectra of the thin films, is seen in Fig. 5 in comparison to the photocurrent spectra of the cell. An illumination from the PcZn side leads to higher I_{SC} especially in the region of the MePTCDI absorption band at about 500 nm, because in this case the MePTCDI electrode is illuminated from the front side. This behaviour agrees with measurements at single MePTCDI electrodes, where a significant decrease of the photocurrent could be found, when front side illumination was replaced by back side illumination. However, at single PcZn electrodes this dependence on the direction of illumination hardly could be found, so that there are no significant differences between the two photocurrent spectra in the region ≥ 600 nm, where only the PcZn thin film absorbs the visible light significantly.

The differences in photocurrent spectra lead to the conclusion that the harvest of the visible light by the tandem cell is higher for an illumination from the PcZn side. Table 3 shows the cell characteristics of the tandem cell for both directions of illumination. As already expected from the photocurrent spectra, the efficiency is higher when the cell is illuminated from the PcZn side. Although the product of I_{SC}, V_{OC} and *FF* for this cell is lower than for the U-tube cell mentioned in Table 1, the overall efficiency of 5.7×10^{-4}% of the tandem cell is higher because only half the area is illuminated in comparison to the cell in Table 1, where each electrode has to be illuminated separately.

The stability of the tandem cell was investigated by illuminating it over a period of 60 h. Over the first 30 h a significant decrease of V_{OC} and I_{SC} occurs, but then these two values remain nearly unchanged at about 30 mV and 4 μA. Underlying an unchanged fill factor, the long time efficiency is only about 0.4×10^{-4}%. The loss in efficiency is running parallel with a decrease of the PcZn film thickness by 17% [11], which was estimated from the decrease of the PcZn absorption maxima in the UV–vis. absorption spectrum of the entire cell, while the thickness of the MePTCDI film remains nearly unchanged.

Table 2. Cell characteristics of ITO/PcZn/electrolyte/MePTCDI/ITO cells (U-tube cells) for various concentrations of the ferri/ferrocyanide electrolyte

Electrolyte concentration mol dm^{-3}	V_{OC} /mV	I_{SC} /μA cm^{-2}	V_{MPP} /mV	I_{MPP} /μA cm^{-2}	*FF*	η /%
4×10^{-4}	205	5.3	80	4.4	0.32	0.000 18
1×10^{-3}	198	7.7	90	5.0	0.30	0.000 23
2×10^{-3}	150	6.2	70	3.7	0.28	0.000 13
5×10^{-3}	95	6.2	40	3.6	0.24	0.000 08
1×10^{-2}	40	4.5	15	2.5	0.21	0.000 02

Both electrodes were illuminated with 96 mW cm^{-2} white light through 460 nm cut-off filters to avoid the influence of different light absorption in the electrolyte

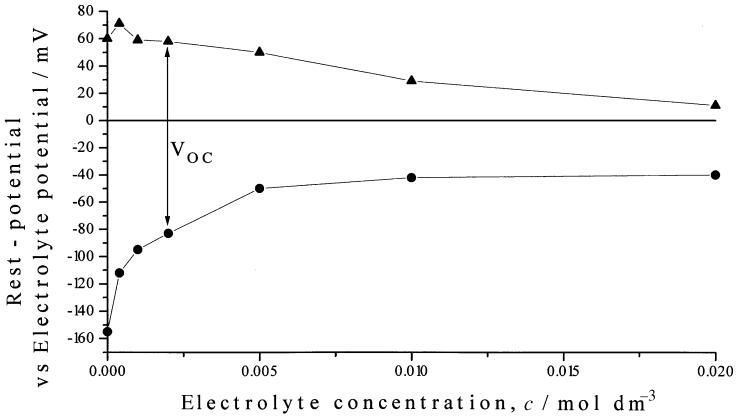

Fig. 4. Concentration dependence of the rest-potentials of (●) MePTCDI and (▲) PcZn electrodes under illumination with 96 mW cm^{-2} white light through 460 nm cut-off filters. The rest-potentials are represented by their differences to the equilibrium redox potential of the electrolyte (230 mV vs SCE) and were determined from the current–voltage curves of the electrodes in a three-electrode setup. V_{OC} as determined for the electrodes in the U-tube cell is also indicated.

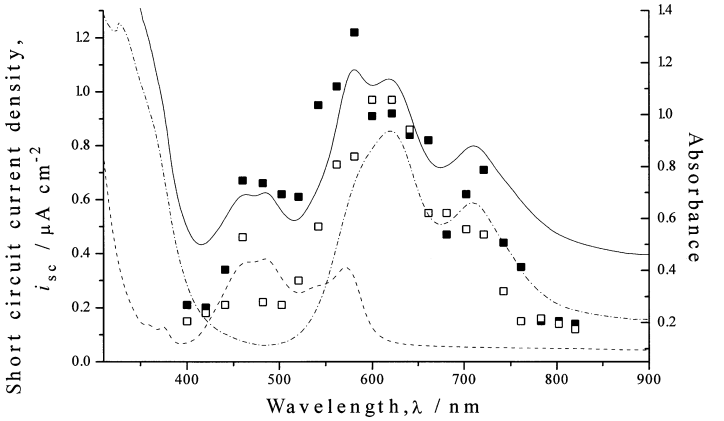

Fig. 5. Spectral dependence of I_{SC} in an ITO/PcZn/ (10^{-3} mol dm^{-3} ferri/ferrocyanide) /MePTCDI/ITO tandem cell for illumination from the MePTCDI side (□) and from the PcZn side (■) in comparison to the absorption spectrum of the entire cell without electrolyte (——). The absorption spectra of the single thin films of MePTCDI (– – – –) and PcZn (—·—·—) are also shown.

4. Discussion

The observed photovoltaic effect, the polarity of the photocurrents as well as the direction and size of the photovoltages, is explained by the positions of HOMO-, LUMO- and Fermi-energies, which are shown in detail for the ferri/ferrocyanide cell in Fig. 6. The cathodic direction (Fig. 1), comparable to reverse bias in a p–n-diode, stands for polarization of the single electrodes, in which significant photocurrents can be observed. The anodic direction corresponds to forward bias conditions of a diode and the power conversion of the incident light can consequently be seen in the lower right hand quadrant. Instead of charge-transport in the heterojunction, however, electrochemical kinetics govern the overall efficiency. The electrode potential of a dark semiconductor or ITO electrode in equilibrium with the ferri/ferrocyanide electrolyte gives its redox potential which can be correlated to the Fermi-energy of the solution $E_{F,electrolyte}$ by

$$E_{F,\,electrolyte} = -4.74\,eV - eE_R \qquad (3)$$

where e is the elementary charge and E_R is the redox potential on the SCE scale [14, 15]. Measurements in a three-electrode setup gave a value of −4.97 eV. The edges of the HOMO band E_V, measured by UV photoelectron spectroscopy (UPS), are given with −5.69 eV for PcZn and −6.84 eV for MePTCDI [2, 3]. The LUMO positions E_C are derived from optical spectra and lead to a gap of 1.65 eV for PcZn and of 2.2 eV for MePTCDI [2]. The positions of the semiconductor Fermi-levels can be derived from the activation energy of the Seebeck coefficient by thermopower measurements. For PcZn a position of E_F of 0.31 eV (at −5.38 eV) above the HOMO and for MePTCDI a position of E_F of 0.14 eV (at −4.78 eV) below the LUMO was determined [4].

Contact of materials of different E_F, which are in this case the two semiconductor electrodes on the one

Table 3. Cell characteristics of ITO/PcZn/electrolyte/MePTCDI/ITO in the tandem cell arrangement for both directions of illumination (96 mW cm^{-2} white light)

Direction of illumination	I_{SC} /μA cm^{-2}	V_{OC} /mV	*FF*	η /%
From MePTCDI side	15.8	91	0.29	0.000 43
From PcZn side	18.3	104	0.29	0.000 57

The electrolyte was ferri/ferrocyanide with a concentration of 10^{-3} mol dm^{-3}

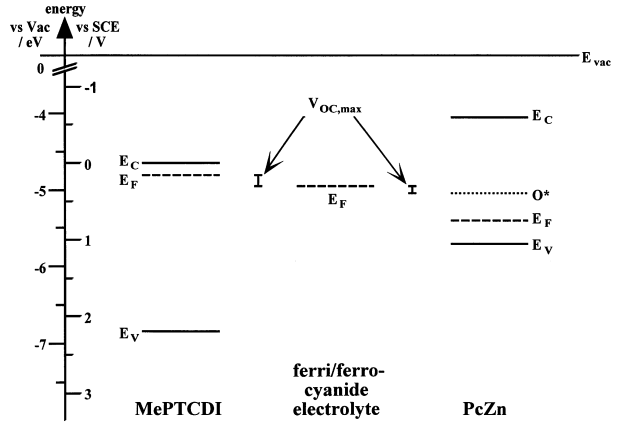

Fig. 6. Energy levels, in particular the HOMO position E_V, the LUMO position E_C and the Fermi-energy E_F, of the different materials used for the photoelectrochemical cell with the ferri/ferrocyanide electrolyte. O* points out the energy level of a surface state caused by oxygen in the PcZn. The value expected for V_{OC} based on the differences in the relevant energy levels is indicated.

hand and the electrolyte on the other hand, leads to the establishment of an electric field and a band bending in the contact region of the semiconductor [14]. By illumination new charge carriers are generated in the molecular semiconductors, which are separated in the electric field. The separation of charge carriers leads to the generation of a photocurrent under short-circuit conditions or to a reduction of the band bending and thus to the building-up of a photovoltage under open-circuit conditions. The positions of the Fermi-levels of MePTCDI above and of PcZn below the Fermi-level of the solution explain the additive behaviour of V_{OC} generated in each electrode (Figure 4). V_{OC} cannot exceed the built-in potential determined by the difference in the Fermi-levels of the materials. This is also the case for the photoelectrochemical cells examined in this study and in accordance with the results shown in Tables 1 and 2. The highest voltages generated by the MePTCDI electrode in the present study are in the range of the difference in the Fermi-levels (MePTCDI and electrolyte) of about 200 mV, though for PcZn V_{OC} never exceeded 60 mV. The latter can be explained by a surface state of the PcZn caused by oxygen 1 eV below the LUMO [16] (at −5.04 eV) which obviously determines the energy of excited charge carriers at the surface of an illuminated PcZn electrode.

In spite of the photovoltages ≤ 205 mV (Tables 1 and 2) which still compare to the values ≤ 415 mV found for all-solid state diodes, the overall efficiency of the photoelectrochemical cells investigated in this study smaller than 6×10^{-4}% by far does not reach the efficiencies as observed in all-solid state devices of up to 0.43% as mentioned above. To our knowledge this is the first direct comparison of organic all-solid state vs photoelectrochemical cells of identical electrodes prepared under the same conditions. When the parameters are compared in detail (Tables 1–3), it is seen that especially I_{SC} is lowered by more than two orders of magnitude (I_{SC} of 18.3 μA in this study compared to an I_{SC} of 3.53 mA in all-solid state devices). At first glance this appears to be surprising as the electrolyte should provide a much larger surface contact area than the contact of two organic polycrystalline films. However, when the charge-transfer kinetics at the electrodes are analysed in more detail, this observation is explained quantitatively.

The photocurrents show a saturation behaviour on reactant concentration, which was shown in Fig. 3. The different behaviour of the photocurrent and the dark current, which increases linearly with the electrolyte concentration, can also explain the changes in V_{OC} seen in Fig. 4. In the dark, the V/I-plots of both PcZn and MePTCDI electrodes cross the V-axis at 230 mV vs SCE, which is the equilibrium redox potential for $K_3Fe(CN)_6/K_4Fe(CN)_6$. When an electrode is illuminated, the intersection is shifted (Figs 2 and 4). The direction of the current in the V-region between the equilibrium potential and the new intersection is opposed to the direction of the current in the dark (Fig. 1). The saturation behaviour of the photocurrent with an increasing electrolyte concentration, while at the same time the dark current increases linearly further on, leads to a decrease of the V-region in which the photocurrent can overcompensate the dark current, hence to a decrease in V_{OC}. In other words, as the currents in the dark and the photocurrent flow in opposite directions, the recombination current at the surface increases with increasing electrolyte concentration.

A saturation with electrolyte concentration, as observed for the photocurrents, is generally not expected in photoelectrochemical reactions. Limitation of the current by diffusion or charge-transfer kinetics would lead to a linear dependence of the current on reactant concentration [15] as it is observed for the dark currents in this study. A saturation is, however, typical for an adsorption reaction. The concentration dependence of the photocurrents is therefore compared to a model which assumes reactant adsorption prior to the charge transfer step as valid for the discussion of the reduction of oxygen at PcZn films [17] and of the oxidation of 2-mercaptoethanol at octacyanophthalocyanine films [18]. Assuming that only adsorbed species react, that the reaction products desorb quickly and that the photocurrent i shows a first order dependence on the concentration c^* of minority carriers at the surface and on the surface coverage Γ by the reactant R, the photocurrent is obtained as

$$i = n F k_f c^* \Gamma \qquad (4)$$

where n is the number of charge carriers transferred to each molecule of reactant, F is the Faraday constant and k_f is the rate constant of the electrochemical reaction. The value of c^* is assumed to be constant at a fixed potential and light intensity. Assuming a Langmuir adsorption equilibrium [15] for R leads to

$$d\Gamma/dt = k(\Gamma_{max} - \Gamma)c_R - k'\Gamma - k_f c^* \Gamma \qquad (5)$$

where k is the rate constant of adsorption, k' is the rate constant of desorption, c_R is the reactant con-

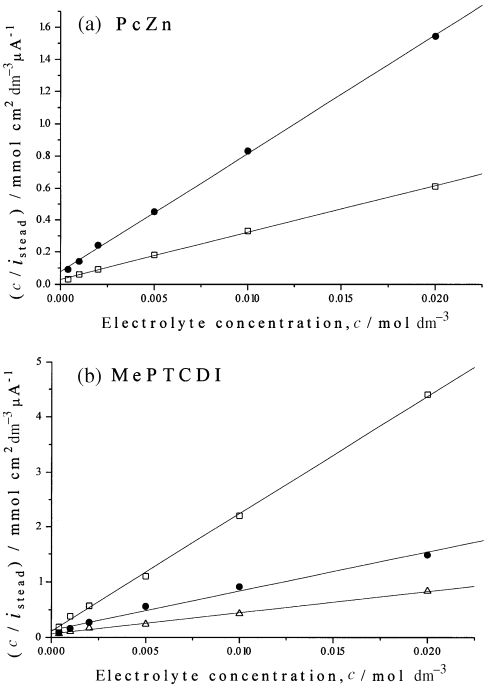

Fig. 7. Plots of experimental data of photocurrents at (a) PcZn and (b) MePTCDI electrodes in a three-electrode setup as dependent on the ferri/ferrocyanide concentration according to Equation 6. The electrode potentials were (□) 50, (●) 240 and (△) 350 mV vs SCE.

centration in the electrolyte and Γ_{max} is the maximum coverage arising from the occupation of all available sites. For the steady-state ($i = i_{stead}$) from Equations 4 and 5 follows

$$c_R/i_{stead} = c_R/i_{max} + [(k'/k) + (k_f c^*/k)]/i_{max} \quad (6)$$

with i_{max} as hypothetical photocurrent arising from Γ_{max}. The plots of c_R/i_{stead} against c_R should therefore yield straight lines for both kinds of electrodes as working electrodes in a three-electrode setup, which is shown in Fig. 7.

Although the validity of the model is obtained for the single electrodes at defined electrode potentials, the linearity arising from Equation 6 could not be found for I_{SC} of a cell consisting of both electrodes (U-tube cell or tandem cell). This is due to the adjustment of the electrode potentials at both electrodes. As the potentials are not defined in this case but are dependent on the different electrolyte concentrations (Figs 2 and 4), the model is not applicable.

5. Conclusions

The p-type semiconducting character of PcZn thin films was confirmed, as well as the n-type character of MePTCDI thin films. PcZn films showed only cathodic photocurrents, while MePTCDI films generated anodic photocurrents. This behaviour is in accordance with the behaviour of the same materials in all-solid state cells. However, in comparison to these cells a much lower efficiency is observed for the photoelectrochemical cell. The low photocurrent obtained for the photoelectrochemical cell was found to be responsible for this result, while the fill factor and the photovoltage are in the same dimension as found for all-solid state cells. The high resistance in the bulk of the thin films, especially of the MePTCDI films, was also shown to influence the behaviour of the entire photoelectrochemical cell, but this factor cannot be responsible for the low efficiency, for then it should also show a reducing influence on the efficiency of all-solid state cells of the same materials.

The reason for the low photocurrent of the photoelectrochemical cells investigated in this study and, consequently, their low efficiency may be attributed to charge-transfer limitation and explained by a model which assumes reactant adsorption prior to the charge transfer step of the surface reaction, which leads to a saturation behaviour of the photocurrent on reactant concentration. Although this model has up to now been used to explain the concentration dependence of irreversible photoelectrochemical reactions like the photoreduction of oxygen at PcZn electrodes, it also proves useful in explaining the photocurrents in a reversible photoelectrochemical cell.

Acknowledgement

The authors are grateful to N.I. Jaeger (Institut für Angewandte und Physikalische Chemie, Universität Bremen) for very helpful cooperation and fruitful discussions and to S. Hiller, E. Karmann, K. Koblitz and J.-P. Meyer for help in sublimation of the samples, thin film preparation and support in technical problems.

References

[1] J. Simon and J.-J. Andre, 'Molecular Semiconductors', Springer, Berlin (1985).
[2] D. Schlettwein, N. R. Armstrong, P. A. Lee and K. W. Nebesny, *Mol. Cryst. Liq. Cryst.* **253** (1994) 161.
[3] D. Schlettwein and N. R. Armstrong, *J. Phys. Chem.* **98** (1994) 11771.
[4] J. P. Meyer, D. Schlettwein, D. Wöhrle and N. I. Jaeger, *Thin Solid Films* **258** (1995) 317.
[5] D. Wöhrle, L. Kreienhoop and D. Schlettwein, *in* 'Phthalocyanines – Properties and Applications' vol. 4 (edited by C. C. Leznoff and A. B. P. Lever), VCH, New York (1996).
[6] D. Wöhrle, L. Kreienhoop, G. Schnurpfeil, J. Elbe, B. Tennigkeit, S. Hiller and D. Schlettwein, *J. Mater. Chem.* **5**(11) (1995) 1819.
[7] D. Schlettwein, N. I. Jaeger and D. Wöhrle, *Ber. Bunsenges. Phys. Chem.* **95**(11) (1991) 1526.
[8] D. Schlettwein, M. Kaneko, A. Yamada, D. Wöhrle and N. I. Jaeger, *J. Phys. Chem.* **95** (1991) 1748.
[9] J. Danziger, J. P. Dodelet, P. Lee, K. W. Nebesny and N. R. Armstrong, *Chem. Mater.* **3** (1991) 821.
[10] G. Tamizhmani, J. P. Dodelet, R. Côté and D. Gravel, *ibid.* **3** (1991) 1046.
[11] A. K. Sobbi, D. Wöhrle and D. Schlettwein, *J. Chem. Soc. Perkin Trans. 2* (1993), 481.
[12] T. J. Klofta, J. Danziger, P. Lee, J. Pankow, K. W. Nebesny and N. R. Armstrong, *J. Phys. Chem.* **91** (1987) 5646.
[13] H. Yanagi, M. Ashida, Y. Harima and K. Yamashita, *Chem. Lett.* (1990), 358.
[14] Y. V. Pleskov, 'Solar Energy Conversion – A Photoelectrochemical Approach', Springer, Berlin (1992).
[15] A. J. Bard and L. R. Faulkner, 'Electrochemical Methods', J. Wiley & Sons, New York (1980).
[16] R. O. Loutfy and L. F. McIntyre, *Can. J. Chem.* **61** (1983) 72.
[17] D. Schlettwein and N. I. Jaeger, *J. Phys. Chem.* **97** (1993) 3333.
[18] E. Karmann, D. Schlettwein and N. I. Jaeger, *J. Electroanal. Chem.* **405** (1996) 217.